Crack Initiation and Propagation in a Pearlitic Nodular Iron Joint Welded with a Nickel-Iron Electrode

The Moiré fringe method and scanning electron microscope examination help to determine reasons for cracking in the weld joint

BY X. -Y. ZHANG, Z. -F. ZHOU, S. -L. WU AND L. -Y. GUAN

ABSTRACT. ENiFe-CI electrodes are widely used in industry for welding QT600-3 nodular iron. Nevertheless, the tensile strength values of these welded joints are low in comparison to those of the base metal, and they have attracted much attention from research workers. In this paper, the total fields of displacement, strain and stress of these welded joints under the uniaxial tension deformation process are obtained by the Moiré fringe method for the first time. Based on the distribution of strain and stress, the reasons for crack initiation and propagation are discussed. The fracture surfaces in these welded joints were examined by scanning electron microscope. Larger spherical substances distributed on the fracture surface in the crack initiation zone and a change of chemical composition in the partially mixed zone were found. These may be reasons for the welded joint to crack under lower tensile stress. The result of microscopy analysis is in good agreement with the Moiré fringe experiment. These new findings will help to improve the properties of ENiFe-CI electrodes and the strength of the welded joint.

Introduction

Many forged steel and cast steel parts can be replaced by lower cost pearlitic nodular iron QT600-3, so it is widely used in the automobile, tractor and other manufacturing industries. Also, welding has been found to be an economical process to repair discontinuities that are sometimes present in casting production, to fix cracked parts, and to join castings to other parts.

In recent years, many methods and materials for welding nodular iron were developed, but most of the repairs and assemblies of nodular iron have utilized ENiFe-CI electrodes. These electrodes appear to have given the best results from the standpoint of both mechanical properties and hot cracking resistance (Refs. 1, 2). Nevertheless, even with these electrodes, the tensile strength values of as-welded joints of QT600-3 nodular iron are lower than those of the base metal (Refs. 3, 4). Some research workers attempted to improve the strength of these welded joints by postweld heat treatment (annealing or normalizing), but results were unsatisfactory (Refs. 3, 5, 6). Therefore, there is an urgent need to find out the reasons for fracturing in these welded joints.

KEY WORDS

Nodular Iron
ENiFe-CI Electrode
Welded Joint
Strain Analysis
Stress Analysis
Fracture Analysis
Crack Initiation
Moiré Fringe Method

X. -Y. ZHANG is a Ph.D. Candidate, Z. -F. ZHOU is a Professor, S. -L.WU is Lecturer and L. -Y. GUAN is Senior Engineer, Jilin University of Technology, Changchun, China.

Experimental Materials and Method

Experimental Materials

The test plates used are pearlitic nodular iron QT600-3. Its chemical composition is shown in Table 1. The experimental electrode is an ENiFe-CI electrode, and its diameter is 3.2 mm (0.125 in.). The chemical composition of deposited metal is shown in Table 2. The density of the Moiré fringe grid is 100 lines/mm, and the size of the grid is 80 X 15 mm.

Preparing Specimen

The joint was made by a shielded metal arc multipass welding process as shown in Fig. 1. The experimental welding machine was operated on AC at 120 A. The welding speed was 2.5 mm/s (0.1 in./s). The mechanical properties of the nodular iron and the deposited metal are shown in Table 3. The specimen was cut along the transverse direction of the welded plate and machined into lath form. Its size is shown in Fig. 2. The Moiré fringe grid was placed on the joint of the specimen.

Experimental Devices and Measuring System

The photographs of the Moiré fringe curve in the tensile specimen were obtained by a Moiré fringe experimental machine. The original data were measured by a JTT-50 projective device. The microstructure of the welded joint and the fracture analysis were examined with an AMARY-1000B scanning electron microscope.

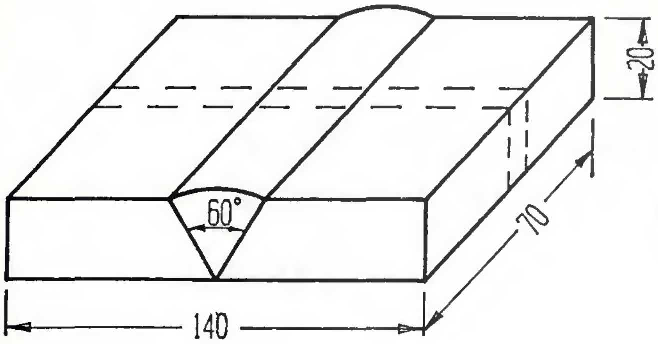

Fig. 1 — Schematic of the welded plate (mm).

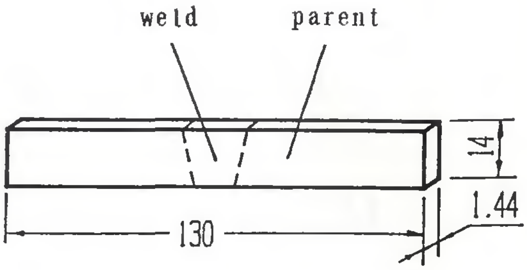

Fig. 2 — Schematic of the tensile specimen (mm).

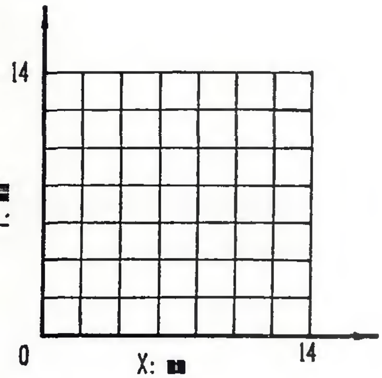

Fig. 3 — Calculation model.

Table 1—Chemical Composition of the Nodular Iron QT600-3, wt-%

C	Si	S	Mn	Mg	ΣRe	Fe
3.10	3.06	0.022	0.60	0.031	0.037	Bal.

Table 2—Chemical Composition of the Deposited Metal, wt-%

C	Si	Ti	Nb	Co	Y	Al	Ni	Fe
1.91	1.18	0.57	0.25	0.42	0.003	0.24	46.20	49.23

Table 3—Mechanical Properties of the Materials

material	yield strength, σ_s MPa	tensile strength, σ_b MPa	elastic modulus, E MPa	poisson's ratio, ν	elongation, δ %
QT600-3	420	640–680	180,000	0.28	2.5–3.5
ENiFe-CI electrode	340	600	160,000	0.32	8–9

Method of Analyzing Data

The study of the crack in the welding specimen under the uniaxial tension deformation process is an elastic-plastic deformation problem. According to the Prandtl-Reuss theory (Refs. 7, 8), when material is in the plastic state, the relationship between stress and strain is nonlinear, the total strain increment during the plastic deformation period is equal to the elastic strain increment plus the plastic strain increment, and the elastic increment is satisfied with the generalized Hooke's law, while the plastic strain increment coincides with Levy-Mises increment theory. If we can obtain the elastic and plastic strain increment on the basis of the appropriate theory, the solution in every case can be obtained. Then, by the Prandtl-Reuss theoretical expression (Ref. 3):

$$de_{ij} = de^{e}_{ij} + de^{p}_{ij}$$

where de_{ij} = total strain increment deviation de^{e}_{ij}; and de^{p}_{ij} = elastic and plastic part of total strain increment deviation, respectively, the solution of the elastic and plastic problem can be acquired.

Because the deformation of the welding specimen under the uniaxial tension process is symmetrical along the center-

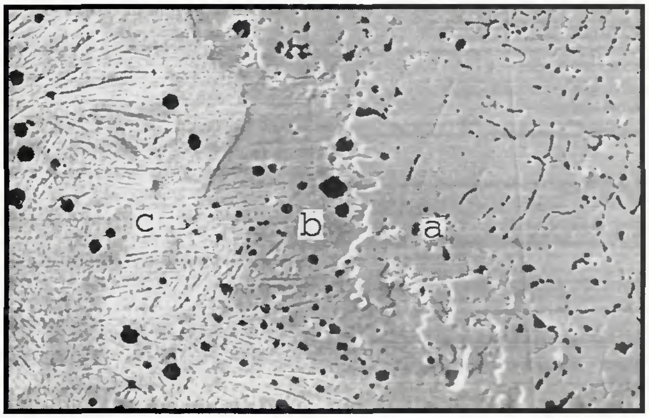

Fig. 4 — Transverse section of the welded joint. A — Weld metal; B — partially mixed

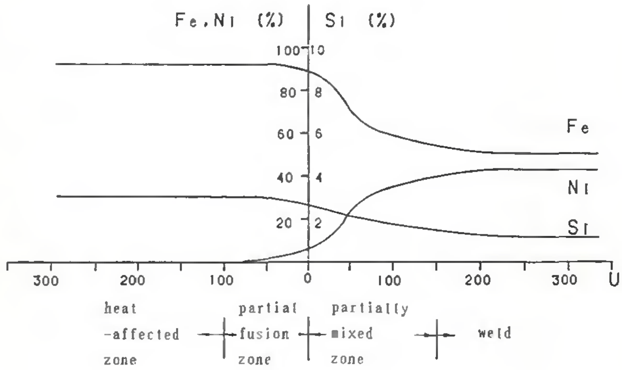

Fig. 5 — The composition distribution of the alloying elements across the welded joint.

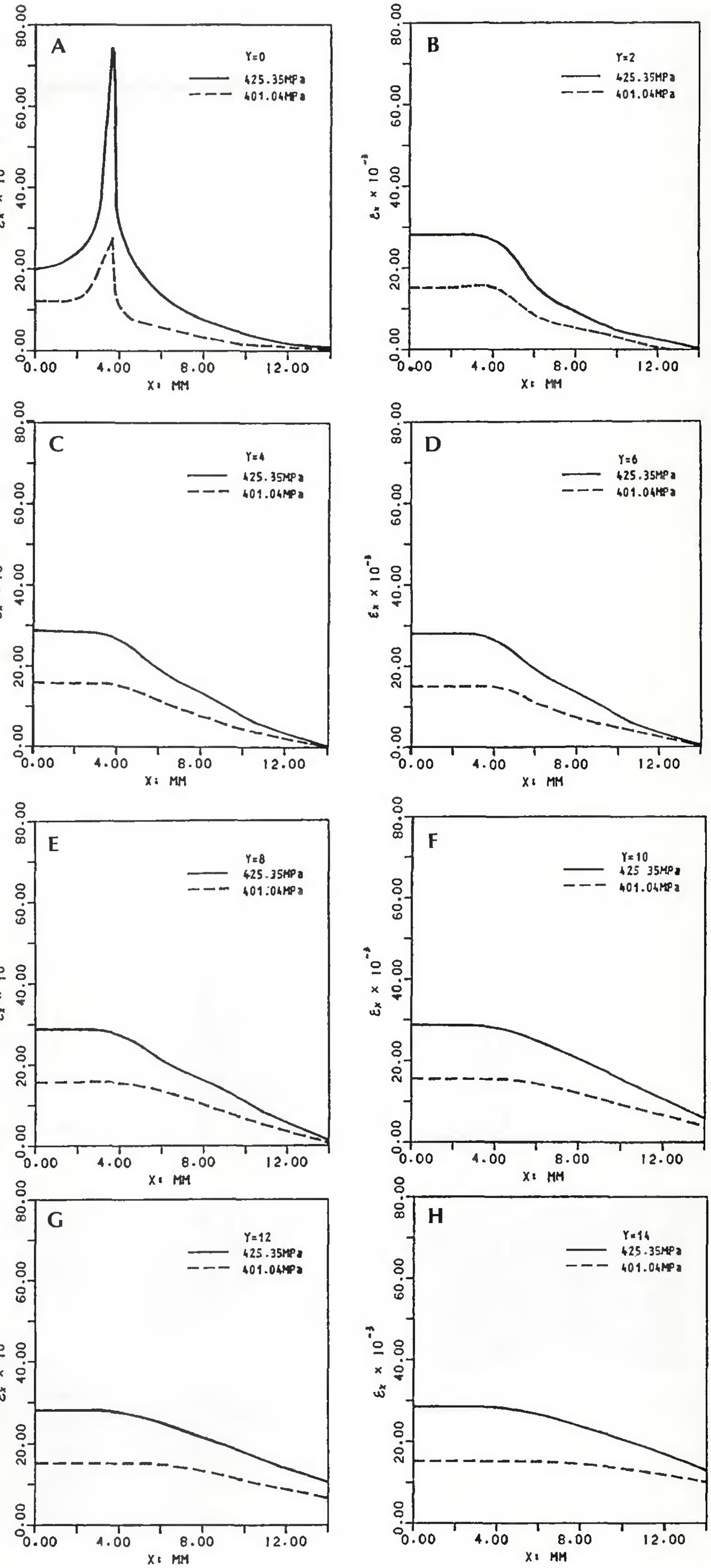

Fig. 6 — The changes of transverse strain on all sections under 401.04 and 425.35 MPa tensile stress.

line of the weld transverse section, we took half of a specimen for analysis. X is the direction of specimen tension, and Y is the centerline of the weld transverse section. The calculating model is shown in Fig. 3.

Experimental Results and Discussion

Microstructure and Chemical Composition across Welded Joint

The joint of QT600-3 nodular iron welded with a ENiFe-Cl electrode is a heterogeneous body, which consists of weld, partially mixed zone, partial fusion zone, heat-affected zone and base metal, as shown in Fig. 4. Figure 5 shows the composition distribution of the alloy element across the welded joint as determined by using EPMA techniques. In the weld, the distribution of iron, nickel and silicon is even, but in the partially mixed zone, the uneven distribution of iron, nickel and silicon is obvious.

Strain Analysis

Figure 6 shows the distribution of transverse strain ε_x on all sections under 401.04 and 425.35 MPa (58.16 and 61.68 ksi) tensile stress, respectively. From the figure, we can see that along the X axis, transverse strain ε_x changes evenly at the beginning, and it is constant. When X is bigger than 4 mm (0.16 in.), the transverse strain decreases, reducing the ε_x value. If the Y value is different, the extent of the reduction in the ε_x value is different, *i.e.*, the slope of the curve is different. With the increase of Y value, the ε_x reduction is slowed, *i.e.*, the slope of the curve becomes slight. On the same section, the ε_x value increases with the increase in tensile stress. But on the section in which Y equals zero, the uneven distribution of transverse strain is obvious, especially when X is bigger than 3 mm and smaller than 4 mm, *i.e.*, near the root of the weld, the peak value for ε_x appears. And with the increase of load, the peak value increases. The analysis of why it happens is stated below.

The welding material is a ENiFe-Cl electrode, which contains 46.20 wt-% Ni and 49.23 wt-% Fe. The base metal is QT600-3 nodular iron. When this kind of electrode is used to weld the nodular iron, the properties of the weld metal and the base metal are different. The weld metal is composed of an austenitic

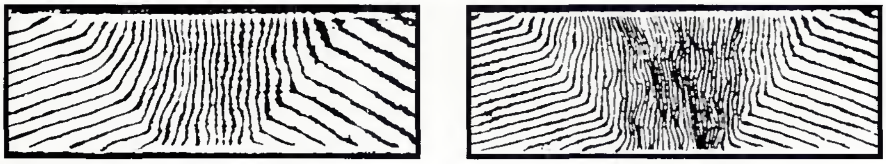

Fig. 7 — The Moiré fringe photographs under 388.89 and 425.35 MPa tensile stress. A — 388.89; B — 425.35.

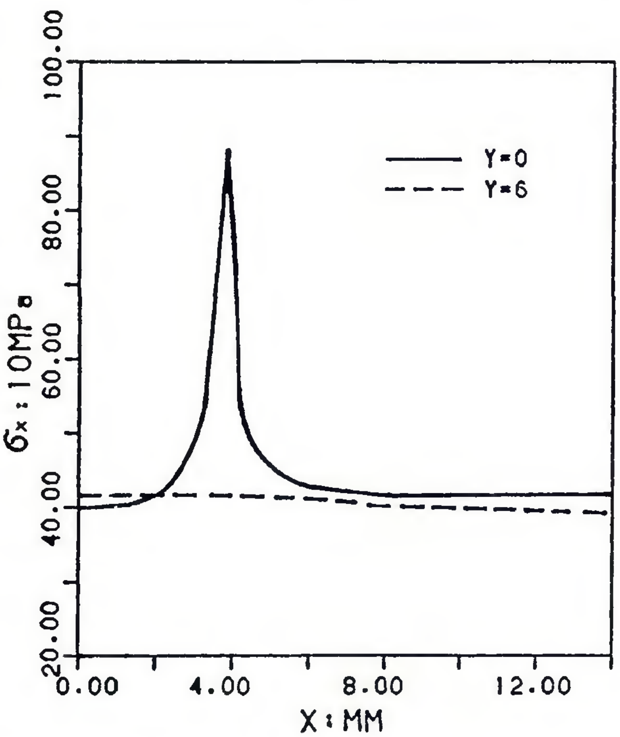

Fig. 8 — The change of transverse stress on the two sections under 425.35 MPa tensile stress.

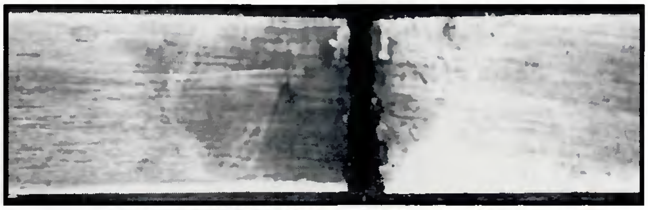

Fig. 9 — Photograph of the tensile specimen crack.

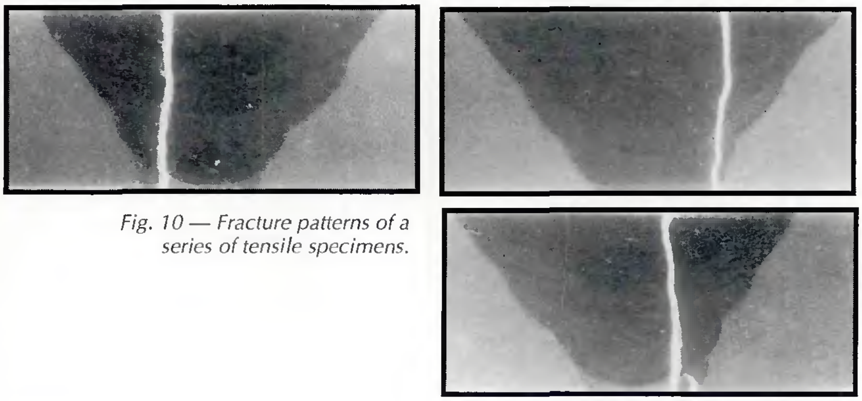

Fig. 10 — Fracture patterns of a series of tensile specimens.

alloy with a yield strength, σ_x, of 340 MPa (49 ksi) and an elongation, δ, of 8–9%, while the σ_x value of the base metal is 420 MPa (61 ksi) and δ is 2.5–3. 5%. The plasticity of the weld is better than that of the base metal, so it easily deforms. Also, the yield strength of the weld metal is lower than that of the base metal; therefore, it yields easily. So under the uniaxial tension deformation process, the Moiré fringe in the weld becomes dense, as shown in Fig. 1, and with the increase of the tensile stress, the Moiré fringe in the weld becomes more dense, since the transverse strain ε_x of the weld is higher than that of the base metal. As the tested tensile specimen is thin and the weld is trapezoidal the unit deformation quantity at the top of the weld is smaller than that at the bottom of the weld when the deformation quantity is constant. Therefore, it is easy to understand why the peak value ε_x appears in the root of the weld metal, as shown in Fig. 6A.

Stress Analysis

Figure 8 shows the changes of transverse stress σ_x on the two sections under 425.35 MPa tensile stress. When Y equals zero in the area where X equals 3.8 mm, *i.e.*, in the area of peak value of ε_x, the peak value of σ_x also appears and reaches 882.6 MPa (128 ksi). Thus the stress in this area concentrates so seriously that it is higher than the tensile strength of the material. Although the crack is invisible to the naked eye, the microcrack initiated needs a certain amount of energy for propagation. Because there exists a plastic area at the tip of the crack, the propagation of the crack will produce the plastic deformation, which will lead to deformation hardening. If it continues to deform, the stress must be increased, *i.e.*, with the propagation of the crack, and plastic deformation is much more difficult, so the stress that the crack needs to continue propagating is higher. The crack propagation is always along the direction that consumes the minimum energy. Suppose that the nominal stress on the transverse section is σ_0. Then that on the fusion face σ_α equals $\sigma_0 \cos^2 \alpha$ and σ_α is obviously lower than σ_0; thus, the specimen should crack vertically along the section in which X equals 3. 8 mm. The experiment shows that when the tensile stress reaches 439.0 MPa (63.7 ksi), the specimen breaks vertically, as shown in Fig. 9.

Fracture Appearance

Experiments on a series of tensile specimens were made with the Moiré fringe method, the fracture patterns of

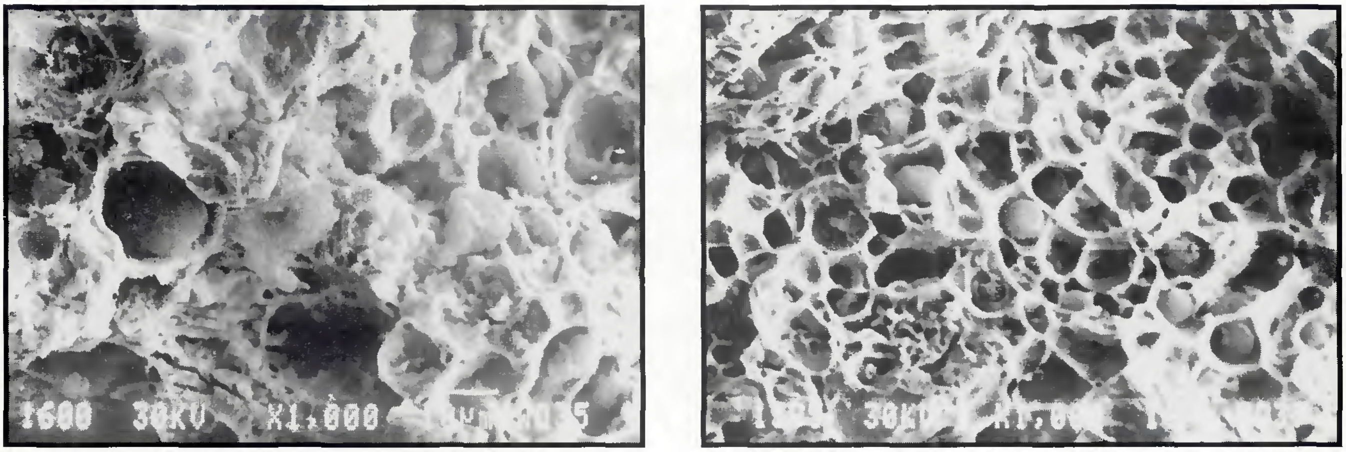

Fig. 11 — Scanning electron microscope images of the fracture surfaces.

which are shown in Fig. 10. We find that the cracks in the specimens always initiate at the root of the weld and propagate vertically in the uniaxial tensile direction, and the tensile strength only reaches 390–440 MPa (56.6–63.8 ksi). The fracture surface was observed with a scanning electron microscope. On the fracture surfaces, a chevron pattern was observed with the apex of the chevron points in the direction from which the crack originated. The root of the weld is the origin.

A lot of dimple rupture is distributed on the fracture surface — Fig. 11. The size of the dimples range from 2 to 20 μm, and there is a spherical substance in every dimple (a partial spherical substance attaches on the other side of the fracture). So the fracture of the tensile specimen begins in the area of the accumulated microdimples as seen in the microscopic view. Because the Fe and Si contents in the partially mixed zone are much higher than those in the weld, as shown in Fig. 5, the partially mixed zone consists of a large amount of nodular graphite and $(FeNi)_3$ C, the size of which is large, as shown in Fig. 4B. Also, we can draw an inference from the comparison of chemical compositions of deposited metal and base metal (as shown In Tables 1 and 2) that the contents of the strengthening elements Ti and Nb in the partially mixed zone are lower than those in the weld metal, but the content of the element C is higher. So actually the crack may initiate at the partially mixed zone of the weld root. The dimple size in the crack initiation zone is much larger than in other areas, as shown in Fig. 11A. When the crack propagates from the partially mixed zone to the weld, the dimple size of the fracture becomes smaller, and the dimples are distributed evenly — Fig. 11B . Further study will focus on this problem.

Conclusions

1) The total fields of displacement, strain and stress of the pearlitic nodular iron joint welded with ENiFe-CI electrodes under the uniaxial tension deformation process were obtained by the Moiré fringe method.

2) Because the mechanical properties of the base metal are different from those of the weld metal, the strain and stress of the welded joint under the uniaxial tension deformation process concentrate at the weld root, which is the one of the reasons for weld joint cracking.

3) Other reasons leading to cracking in the weld joint may be the great amount of large spherical substances distributed on the fracture surface and the change of chemical composition in the partially mixed zone.

References

1. Stewart, J. P. 1981. *The Welder's Handbook.* Reston Publishing Co., Inc.

2. *Welding Handbook*, Seventh Edition, Vol. 4. 1983. The American Welding Society, Miami, Fla.

3. Flannery, J. W. 1968. Welding ductile iron —part one. *Welding Engineer*, (11).

4. Bishel, R. A., Conaway, H. R. 1976. Flux cored arc welding for high-quality joints in ductile iron. *AFS Transactions*, (4).

5. Ball, F. A., *et al.* 1954. Metallic arc welding of spheroidal graphite cast iron. *Foundry Trade Journal*, (10).

6. Voigt, R. C., and Loper, C. R. 1986. Welding metallurgy of gray and ductile cast irons. *AFS Transactions.*

7. Bing, S., *et al.* Measuring and calculating the plastic stress deformation by the Moiré fringe method. *Proceeding of the Third Annual Meeting of Forging Insititute of China Mechanical Engineering Society.*

8. Bing, S. 1985. The Moiré fringe experimental analysis of the plastic material stress and strain. *Scientific Report of Qing Hua University.*

Stress Indexes, Pressure Design and Stress Intensification Factors for Laterals in Piping

WRC Bulletin 360
January 1991

By E. C. Rodabaugh

The study described in this report was initiated in 1987 by the PVRC Design Division Committee on Piping, Pumps and Valves under a PVRC grant to E. C. Rodabaugh following an informal request from the ASME Boiler and Pressure Vessel Committee, Working Group on Piping (WGPD) (SGD) (SC-II) to develop stress indexes and stress intensification factors (*i*-factors) for piping system laterals that could be considered by the ASME Committee for incorporation into the code.

In this study, the author has considers all existing information on lateral connections in concert with existing design guidance for 90-deg branch connections; and has developed compatible design guidance for lateral connections for piping system design. As a corollary bonus, he has also extended the parameter range for the "B" stress indexes for 90-deg branch connections from d/D = 0.5 (the present code limit) to d/D = 1.0. Therefore, this report should be of significant interest to the B31 industrial piping code committees, as well as the ASME Boiler and Pressure Vessel Committee.

Publication of this bulletin was sponsored by the Committee on Piping, Pumps and Valves of the Design Division of the Pressure Vessel Research Council. The price of WRC Bulletin 360 is $30.00 per copy, plus $5.00 for U.S. and $10.00 for overseas, postage and handling. Orders should be sent with payment to the Welding Research Council, Room 1301, 345 E. 47th St., New York, NY 10017.

WRC Bulletin 361
February 1991

This Bulletin contains two reports that compare the French RCC-M Pressure Vessel Code and the U.S ASME Section III Code on Design of Nuclear Components and Piping Design Rules.

(1) Improvements on Fatigue Analysis Methods for the Design of Nuclear Components Subjected to the French RCC-M Code

By J. M. Grandemange, J. Heliot, J.Vagner, A. Morel and C. Faidy

(2) Framatome View on the Comparison between Class 1 and Class 2 RCC-M Piping Design Rules

By C. Heng and J. M. Grandemange.

Publication of this bulletin was sponsored by the Pressure Vessel Research Council of the Welding Research Council. The price of WRC Bulletin 361 is $30.00 per copy, plus $5.00 for U.S. and $10.00 for overseas, postage and handling. Orders should be sent with payment to the Welding Research Council, Room 1301, 345 E. 47th St., New York, NY 10017.